2009 American Control Conference
Hyatt Regency Riverfront, St. Louis, MO, USA
June 10-12, 2009

Actuator Fault Detection and Reconfiguration in Distributed Processes with Measurement Sampling Constraints

Sathyendra Ghantasala and Nael H. El-Farra[†]
Department of Chemical Engineering & Materials Science
University of California, Davis, CA 95616 USA

Abstract— **This work develops a model-based approach for the detection and compensation of actuator faults in distributed processes described by parabolic PDEs with a limited number of measurements that are sampled at discrete time instances. Using an approximate finite-dimensional system that captures the dominant dynamics of the PDE, an observer-based output feedback controller that stabilizes the closed-loop system in the absence of faults is initially designed. The observer estimates are also used for fault detection by comparing the output of the observer with that of the process, and using the discrepancy as a residual. To compensate for measurement unavailability, a model of the approximate finite-dimensional system is embedded within the controller to provide the observer with estimates of the output measurements between sampling instances. The state of the model is then updated using the actual measurements whenever they become available from the sensors. By formulating the closed-loop system as a combined discrete-continuous system, an explicit characterization of the minimum allowable sampling rate that guarantees both closed-loop stability and residual convergence in the absence of faults is obtained in terms of the model accuracy, the controller design parameters and the spatial placement of the control actuators. This characterization is used as the basis for deriving (1) a time-varying threshold on the residual which can be used to detect faults for a given sampling period, and (2) an actuator reconfiguration law that determines the set of feasible fall-back actuators that preserve closed-loop stability under a given measurement sampling rate. Finally, the implementation of the fault detection and fault-tolerant control architecture on the infinite-dimensional system is analyzed using singular perturbations, and the results are demonstrated using a diffusion-reaction process example.**

I. Introduction

Distributed parameter systems such as transport-reaction processes and fluid flow systems are modeled by systems of Partial Differential Equations (PDEs). While these systems have been the subject of active research within process control over the past few decades (e.g., see [1], [2], [3], [4], [5], [6] and the references therein), the development of systematic methods for the diagnosis and handling of faults in distributed control systems has received only limited attention. This is an important problem given the vulnerability of automated control systems to malfunctions in the control actuators, measurement sensors and process equipment, as well as the increasingly stringent requirements placed on safety and reliability in industrial process operation. Most of the available results on this problem have focused on spatially homogeneous processes modeled by systems of ordinary differential equations (e.g., see [7], [8], [9], [10], [11], [12], [13] and the references therein). Examples of existing results for distributed parameter systems include methods for fault detection and accommodation based on approximate linear or nonlinear models (e.g., [14], [15]), as well as reconfiguration-based fault-tolerant control (FTC) of nonlinear distributed processes [16]. Recently, we developed in [17], [18] a unified framework for the integration of model-based fault detection (FD), isolation and control system reconfiguration for distributed processes modeled by nonlinear parabolic PDEs with control constraints and actuator faults. Practical implementation issues such as the presence of plant-model mismatch and the availability of measurements at a finite number of locations along the spatial domain were subsequently addressed in [19].

Beyond the problems of uncertainty and constraints, one of the key issues that needs to be accounted for in the design of monitoring and fault-tolerant control systems is the issue of measurement sampling. In practice, measurements of the process outputs are typically available from the sensors at discrete time instances and not continuously. The frequency at which the measurements are available is dictated by the sampling rate which is typically constrained by the inherent limitations on the data collection and processing capabilities of the measurement sensors. The limitations on the frequency of measurement availability imposes restrictions on the implementation of the feedback controller and can also erode the diagnostic and fault-tolerance capabilities of the fault-tolerant control architecture if not explicitly accounted for at the design stage. Within the feedback control layer, for example, infrequent measurement sampling could result in substantial errors in the implemented control action leading to possible loss of stability or performance degradation. The lack of frequent measurements also limits our ability to accurately monitor the trajectory of the process variables rendering it difficult to evaluate the residuals or diagnose faults. At the control reconfiguration level, knowledge of how a given control configuration (i.e., the spatial placement of actuators and sensors) depends on the sampling rate is critical for identifying the appropriate backup configuration that should be activated following fault detection to maintain closed-loop stability.

Motivated by these considerations, we develop in this work a fault detection and fault-tolerant control structure for distributed processes modeled by parabolic PDEs with a limited number of measurements that are sampled at

[†] To whom correspondence should be addressed: E-mail: nhelfarra@ucdavis.edu. Financial support by ACS-PRF grant, 47072-G9, is gratefully acknowledged.

978-1-4244-4524-0/09/$25.00 ©2009 AACC

discrete time instances. The structure consists of a family of output feedback controllers, observer-based fault detection filters that account for the discrete sampling of measurements and a switching law that orchestrates the transition from the faulty actuator configuration to a healthy fall-back following fault detection. A key idea is to embed within the fault-tolerant control system an approximate model of the dominant process dynamic modes to provide the observers with estimates of the output measurements between sampling instances, and to update the state of the model using the actual measurements whenever they become available from the sensors at the discrete sampling times. The rest of the paper is organized as follows. Following some preliminaries in Section II, an approximate finite-dimensional system is obtained using modal decomposition techniques and then used in Section III to construct the model-based FD-FTC structure. The sampled-data closed-loop system is then formulated as a discrete jump system, and an explicit characterization of the minimum allowable sampling rate that guarantees both closed-loop stability and residual convergence in the absence of faults is obtained. This characterization is then used as the basis for deriving appropriate fault detection and actuator reconfiguration laws for a given sampling rate. A singular perturbation formulation is used in Section IV to derive precise conditions for the implementation of the finite-dimensional FD-FTC architecture on the infinite-dimensional system. Finally, in Section V the proposed methodology is applied to achieve fault-tolerant stabilization of an unstable steady-state of a representative diffusion-reaction process.

II. Preliminaries

A. Class of systems

We consider spatially-distributed processes modeled by linear parabolic PDEs of the form:

$$\frac{\partial \bar{x}}{\partial t} = \alpha \frac{\partial^2 \bar{x}}{\partial z^2} + \beta \bar{x} + \omega \sum_{i=1}^{m} b_i^k(z)[u_i^k(t) + f_{a_i}^k(t)] \quad (1)$$

$$k \in \mathcal{K} := \{1, 2, \cdots, N\}, \; N < \infty \quad (2)$$

$$y_l(t) = \int_0^{\pi} q_l(z)\bar{x}(z,t)dz, \; l = 1, \cdots, n \quad (3)$$

subject to the boundary and initial conditions:

$$\bar{x}(0,t) = \bar{x}(\pi,t) = 0, \; \bar{x}(z,0) = \bar{x}_0(z) \quad (4)$$

where $\bar{x}(z,t) \in \mathbb{R}$ denotes the process state variable, $z \in [0,\pi] \subset \mathbb{R}$ is the spatial coordinate, $t \in [0,\infty)$ is the time, u_i^k denotes the i-th manipulated input (control actuator) associated with the k-th control actuator configuration, $b_i^k(\cdot)$ is a function that describes how the control action is distributed in $[0,\pi]$, $f_{a_i}^k$ describes a fault in the i-th actuator of the k-th configuration, $y_l(t) \in \mathbb{R}$ is a measured output, $q_l(\cdot)$ is a function that describes how the measured output is distributed in $[0,\pi]$, the parameters $\alpha > 0, \beta, \omega$ are constants, and $\bar{x}_0(z)$ is a smooth function of z.

Throughout the paper, the notations $\|\cdot\|$ and $\|\cdot\|_2$ will be used to denote the L_2 norms associated with a finite-dimensional and infinite-dimensional Hilbert spaces, respectively. Furthermore, a bounded linear operator $\mathcal{N}$ is said to be power-stable if there exists positive real numbers β and γ such that $\|\mathcal{N}^j\| \leq \beta e^{-\gamma j}$, for any non-negative integer j. The spectral radius of a bounded linear operator $\mathcal{N}$ is defined as $r(\mathcal{N}) = \lim_{j\to\infty} \|\mathcal{N}^j\|^{1/j} \leq \|\mathcal{N}\|$. From these definitions, it can be verified that $\mathcal{N}$ is power-stable if and only if $r(\mathcal{N}) < 1$. Finally, the notation $x(t_j^-)$ will be used to denote the limit $\lim_{t\to t_j^-} x(t)$.

For a precise characterization of the class of PDEs considered in this work, we formulate the PDE of Eqs.1-4 as an infinite-dimensional system in the state space $\mathcal{H} = L_2(0,\pi)$, with inner product $\langle \omega_1, \omega_2 \rangle = \int_0^{\pi} \omega_1(z)\omega_2(z)dz$, and norm $\|\omega_1\|_2 = \langle \omega_1, \omega_1 \rangle^{\frac{1}{2}}$, where ω_1, ω_2 are two elements of $L_2(0,\pi)$. Defining the input and output operators as $\mathcal{B}^k u^k = \omega \sum_{i=1}^{m} b_i^k(\cdot)u_i^k$, $\mathcal{Q}x = [\langle q_1, x\rangle \; \langle q_2, x\rangle \cdots \langle q_n, x\rangle]'$, the system of Eqs.1-4 can be written in the following form:

$$\begin{aligned} \dot{x}(t) &= \mathcal{A}x(t) + \mathcal{B}^k[u^k(t) + f_a^k(t)], \; x(0) = x_0 \quad (5) \\ y(t) &= \mathcal{Q}x(t) \quad (6) \end{aligned}$$

where $x(t)$ is the state function defined on an appropriate Hilbert space, $\mathcal{A}$ is the differential operator, $u^k = [u_1^k \; u_2^k \; \cdots \; u_m^k]'$, $f_a^k = [f_{a_1}^k \; f_{a_2}^k \; \cdots \; f_{a_m}^k]'$, $y = [y_1 \; y_2 \; \cdots, y_n]'$ and $x_0 = \bar{x}_0(z)$. For $\mathcal{A}$, the solution of the eigenvalue problem ($\mathcal{A}\phi_j = \lambda_j \phi_j, \; j = 1, \ldots, \infty$), where λ_j denotes an eigenvalue and ϕ_j denotes an eigenfunction, yields real and ordered eigenvalues. Also, for a given α and β, only a finite number of unstable eigenvalues exist, and the distance between two consecutive eigenvalues (i.e., λ_j and λ_{j+1}) increases as j increases. Furthermore, for parabolic PDEs, the spectrum of $\mathcal{A}$ can be partitioned, where $\sigma_1(\mathcal{A}) = \{\lambda_1, \cdots, \lambda_m\}$ contains the first m (with m finite) "slow" eigenvalues and $\sigma_2(\mathcal{A}) = \{\lambda_{m+1}, \lambda_{m+2}, \cdots\}$ contains the remaining "fast" stable eigenvalues where $|\lambda_m|/|\lambda_{m+1}| = O(\epsilon)$ and $\epsilon < 1$ is a small positive number characteristic of the large separation between the slow and fast eigenvalues of $\mathcal{A}$. This implies that the dominant dynamics of the PDE can be described by a finite-dimensional system, and motivates the use of modal decomposition in the next subsection to derive a finite-dimensional system that captures the dominant (slow) dynamics of the PDE.

B. Modal decomposition

Let $\mathcal{H}_s$, $\mathcal{H}_f$ be modal subspaces of $\mathcal{A}$, defined as $\mathcal{H}_s = \text{span}\{\phi_1, \ldots, \phi_m\}$ and $\mathcal{H}_f = \text{span}\{\phi_{m+1}, \phi_{m+2}, \ldots\}$. Defining the orthogonal projection operators, $\mathcal{P}_s$ and $\mathcal{P}_f$, such that $x_s = \mathcal{P}_s x$, $x_f = \mathcal{P}_f x$, the state of the system of Eq.5 can be decomposed as $x = x_s + x_f$. Applying $\mathcal{P}_s$ and $\mathcal{P}_f$ and using the decomposition of x, the system of Eqs.5-6 can be decomposed as:

$$\dot{x}_s = \mathcal{A}_s x_s + \mathcal{B}_s^k[u^k + f_a^k], \; x_s(0) = \mathcal{P}_s x_0 \quad (7)$$

$$\dot{x}_f = \mathcal{A}_f x_f + \mathcal{B}_f^k[u^k + f_a^k], \; x_f(0) = \mathcal{P}_f x_0 \quad (8)$$

$$y = \mathcal{Q}x_s + \mathcal{Q}x_f \quad (9)$$

where $\mathcal{A}_s = \mathcal{P}_s\mathcal{A}$ is an $m \times m$ diagonal matrix of the form $\mathcal{A}_s = \text{diag}\{\lambda_j\}$, $\mathcal{B}_s^k = \mathcal{P}_s\mathcal{B}^k$, $\mathcal{A}_f = \mathcal{P}_f\mathcal{A}$ is an unbounded differential operator which is exponentially stable (following from the fact that $\lambda_{m+1} < 0$ and the selection of $\mathcal{H}_s$ and $\mathcal{H}_f$), $\mathcal{B}_f^k = \mathcal{P}_f\mathcal{B}^k$. Neglecting the fast and stable x_f-subsystem of Eq.8, the following approximate, m-dimensional slow system is obtained:

$$\dot{\bar{x}}_s = \mathcal{A}_s\bar{x}_s + \mathcal{B}_s^k[u^k + f_a^k], \ \ \bar{y} = \mathcal{Q}\bar{x}_s \tag{10}$$

where the bar symbols denote that these variables are associated with a finite-dimensional system. To facilitate the controller synthesis and simplify closed-loop analysis, we will consider in the remainder of the paper that the inverse (or pseudo-inverse in the case of a non-square system) of the operator $\mathcal{Q}$ exists. This requirement, which can be met by appropriate choice of the locations of the measurement sensors, allows obtaining estimates of the state of the finite-dimensional system of Eq.10 from the measurements.

III. Design of finite-dimensional sampled-data fault-tolerant control system

A. *Controller synthesis and analysis in the absence of faults*

The objective of this part is to design for each actuator configuration an output feedback controller that enforces (in the absence of faults) closed-loop stability using sampled measurements, and to characterize the minimum allowable sampling rate necessary to guarantee closed-loop stability.

1) Output feedback controller synthesis: We consider an observer-based output feedback controller of the form:

$$u^k = \mathcal{F}^k\eta, \ \ \dot{\eta} = \widehat{\mathcal{A}}_s\eta + \widehat{\mathcal{B}}_s^k u^k + \mathcal{L}(\bar{y} - \mathcal{Q}\eta) \tag{11}$$

where $\mathcal{F}$ is the feedback gain, η is the state of an observer that generates estimates of $\bar{x}_s$ using $\bar{y}$, $\widehat{\mathcal{A}}_s$ and $\widehat{\mathcal{B}}_s^k$ are bounded operators that represent models of $\mathcal{A}_s$ and $\mathcal{B}_s^k$, respectively, and $\mathcal{L}$ is the observer gain. Notice that in general $\widehat{\mathcal{A}}_s \neq \mathcal{A}_s$ and $\widehat{\mathcal{B}}_s^k \neq \mathcal{B}_s^k$ to allow for possible plant-model mismatch. When the output measurements are available continuously, and in the special case that $\widehat{\mathcal{A}}_s = \mathcal{A}_s$, $\widehat{\mathcal{B}}_s^k = \mathcal{B}_s^k$, a necessary and sufficient condition for stability of the closed-loop system of Eqs.10-11 (with $f_a^k \equiv 0$) is to have the eigenvalues of both $\mathcal{A}_s + \mathcal{B}_s^k\mathcal{F}^k$ and $\mathcal{A}_s - \mathcal{L}\mathcal{Q}$ in the left half of the complex plane. When the output measurements are available only at discrete time instances, however, the observer in Eq.11 cannot be implemented directly. One way to deal with this problem is to embed within the controller a dynamic model of the finite-dimensional slow system of Eq.10 to provide the observer with an estimate of the output to be used when measurements are not available from the sensors and to update the state of the model using the actual output measurements whenever they are provided by the sensors at discrete time instances. The model-based output feedback controller is implemented as follows:

$$\begin{array}{rcl} u^k(t) & = & \mathcal{F}^k\eta(t), \ \ t \in (t_j, t_{j+1}) \\ \dot{\eta}(t) & = & \widehat{\mathcal{A}}_s\eta(t) + \widehat{\mathcal{B}}_s^k u^k(t) + \mathcal{L}(\widehat{y}(t) - \mathcal{Q}\eta(t)) \\ \dot{w}(t) & = & \widehat{\mathcal{A}}_s w(t) + \widehat{\mathcal{B}}_s^k u^k(t), \ \ \widehat{y}(t) = \mathcal{Q}w(t) \\ \widehat{y}(t_j) & = & \bar{y}(t_j), \ j = 0, 1, 2, \cdots \end{array} \tag{12}$$

where $\widehat{y}$ is an estimate of $\bar{y}$, w is an estimate of $\bar{x}_s$, $\widehat{\mathcal{A}}_s$ and $\widehat{\mathcal{B}}_s^k$ are bounded operators that model the dynamics of the slow subsystem of Eq.10, and $\Delta := t_{j+1} - t_j$ is the sampling period. Note that since $\mathcal{Q}$ is invertible, re-setting the output of the model to match the actual output is equivalent to re-setting the state of the model since $w(t_j) = \mathcal{Q}^{-1}\bar{y}(t_j)$.

2) Characterizing the minimum allowable sampling rate: To simplify the analysis, we focus on the case when the sampling period is constant and the same for all the sensors, i.e., we require that all sensors communicate their measurements concurrently every Δ seconds. To characterize the maximum allowable sampling period between the sensors and the controller, we define the model estimation error as $\bar{e}_s(t) = w(t) - \bar{x}_s(t)$, where $\bar{e}_s \in \mathcal{H}_s$ represents the difference between the state of the approximate system of Eq.10 and the state of its model given in Eq.12. Defining the augmented state $\chi = [\bar{x}_s \ \eta \ \bar{e}_s]'$ which is an element of the extended state space $\mathcal{H}_s^e = \mathcal{H}_s \times \mathcal{H}_s \times \mathcal{H}_s$, it can be shown that the augmented slow subsystem can be formulated as a combined discrete-continuous system and written in the following operator-matrix form for clarity:

$$\begin{array}{rcl} \dot{\chi}(t) & = & \Lambda_k\chi(t), \ \ t \in (t_j, t_{j+1}) \\ \bar{e}_s(t_j) & = & 0, \ \ j = 0, 1, 2, \cdots, \end{array} \tag{13}$$

where

$$\Lambda_k = \begin{bmatrix} \mathcal{A}_s & \mathcal{B}_s^k\mathcal{F}^k & \mathcal{O} \\ \mathcal{L}\mathcal{Q} & \mathcal{C} & \mathcal{L}\mathcal{Q} \\ \widetilde{\mathcal{A}}_s & \widetilde{\mathcal{B}}_s^k\mathcal{F}^k & \widehat{\mathcal{A}}_s \end{bmatrix} \tag{14}$$

is a bounded linear operator, $\mathcal{C} = \widehat{\mathcal{A}}_s + \widehat{\mathcal{B}}_s^k\mathcal{F}^k - \mathcal{L}\mathcal{Q}$, and $\widetilde{\mathcal{A}}_s = \widehat{\mathcal{A}}_s - \mathcal{A}_s$, $\widetilde{\mathcal{B}}_s^k = \widehat{\mathcal{B}}_s^k - \mathcal{B}_s^k$ represent the modeling errors. Note that while the state of the slow system, $\bar{x}_s$, and the state of the observer, η, evolve continuously in time, the error $\bar{e}_s$ is reset to zero at each transmission instance since the state of the model is updated every Δ seconds using the true output measurement.

In order to derive conditions for closed-loop stability in terms of the sampling period, we need to express the closed-loop response as a function of the sampling period. To this end, it can be shown that the system described by Eq.13 with initial condition $\chi(t_0) = [\bar{x}_s(t_0) \ \eta(t_0) \ 0]' = \chi_0$ has the following solution for $t \in [t_j, t_{j+1})$:

$$\chi(t) = \mathcal{T}_{\Lambda_k}(t - t_j)\left(\mathcal{I}_o\mathcal{T}_{\Lambda_k}(\Delta)\mathcal{I}_o\right)^j\chi_0 \tag{15}$$

with $t_{j+1} - t_j = \Delta$, where $\mathcal{T}_{\Lambda_k}(t) : \mathcal{H}_s^e \to \mathcal{H}_s^e$ is a C_0-semigroup generated by Λ_k on $\mathcal{H}_s^e$, $\mathcal{I}_o = \mathrm{diag}([\mathcal{I} \ \mathcal{I} \ \mathcal{O}])$, $\mathcal{I}$ is the identity operator. Specifically, for $t \in [t_j, \ t_{j+1})$, the augmented system admits the solution $\chi(t) = \mathcal{T}_{\Lambda_k}(t - t_j)\chi(t_j)$. Note that at times t_j, $j = 1, 2, \cdots$, $\chi(t_j) = [\bar{x}_s(t_j) \ \eta(t_j) \ 0]'$ since the error $\bar{e}_s(t)$ is reset to zero. This can be represented by writing $\chi(t_j) = \mathcal{I}_o\chi(t_j^-)$. Since $\chi(t_j^-) = \mathcal{T}_{\Lambda_k}(\Delta)\chi(t_{j-1})$, we have $\chi(t_j) = \mathcal{I}_o\mathcal{T}_{\Lambda_k}(\Delta)\chi(t_{j-1})$. Therefore, given that at $t = t_0$, $\chi(t_0) = \chi_0$ is the initial condition, we have $\chi(t) = \mathcal{T}_{\Lambda_k}(t - t_j)(\mathcal{I}_o\mathcal{T}_{\Lambda_k}(\Delta))^j\chi_0 = \mathcal{T}_{\Lambda_k}(t - t_j)(\mathcal{I}_o\mathcal{T}_{\Lambda_k}(\Delta)\mathcal{I}_o)^j\chi_0$. The following proposition provides a necessary and sufficient condition for stability of the finite-dimensional closed-loop system subject to sampling and in the absence of faults.

Proposition 1: *Consider the closed-loop system of Eq.10 and Eq.12, for a fixed $k \in \mathcal{K}$, with $f_a^k \equiv 0$, and consider the augmented system of Eqs.13-14 whose solution is given by Eq.15. Let $\mathcal{N}_k(\Delta) = \mathcal{I}_o\mathcal{T}_{\Lambda_k}(\Delta)\mathcal{I}_o$. Then the zero solution, $\chi = [\bar{x}_s \ \eta \ \bar{e}_s]' = [0 \ 0 \ 0]'$, is exponentially stable if and only if $r(\mathcal{N}_k(\Delta)) < 1$.*

Proof: Sufficiency can be shown by evaluating the norm of the solution described in Eq.15, which yields $\parallel \chi(t) \parallel \leq$

$\| \mathcal{T}_{\Lambda_k}(t-t_j) \| \| \mathcal{N}_k^j \| \| \chi_0 \|$. From the properties of the linear bounded operator Λ_k, it follows that $\| \mathcal{T}_{\Lambda_k}(t-t_j) \| \leq \varphi_1 e^{\mu(t-t_j)} := \mu_1$, where $\varphi_1 > 0$ and $\mu = \sup\{Re\, \sigma(\Lambda_k)\}$. In general this term can always be bounded since $t - t_j \leq \Delta$. Even if Λ_k has eigenvalues with positive real parts, $\| \mathcal{T}_{\Lambda_k}(t-t_j) \|$ can only grow a certain amount, and this growth is independent of j. The term $\| \mathcal{N}_k^j \|$ is bounded if and only if $\mathcal{N}_k$ is power-stable, i.e., $\| \mathcal{N}_k^j \| \leq \varphi_2 e^{-\gamma j}$, with some $\varphi_2, \gamma > 0$. Since $j = t_j/\Delta$ and $t \in [t_j, t_{j+1})$, this bound can be expressed in terms of t as $\| \mathcal{N}_k^j \| \leq \varphi_3 e^{-\gamma_s t}$, where $\varphi_3 = \varphi_2 e^{\gamma} > 0$ and $\gamma_s = \gamma/\Delta > 0$. Combining all the estimates obtained, we finally arrive at the following bound $\| \chi(t) \| \leq \varphi_4 \| \chi_0 \| e^{-\gamma_s t}$, where $\varphi_4 := \varphi_3 \mu_1 > 0$, which implies that the origin of the system of Eqs.13-14 is exponentially stable. Necessity can be established by analyzing a periodic sample of the response at times t_{j+1}^-, i.e., just before the update, (which should be stable if the system is stable) and then showing that if $r(\mathcal{N}_k(\Delta)) > 1$, $\bar{x}_s(t_{j+1}^-)$ will in general grow with j which contradicts the stability assumption. This argument is conceptually similar to the one presented in [20] except that it involves operators defined over functional spaces. This completes the proof.

Remark 1: It can be seen from the structure of Λ_k in Eq.14 that the minimum stabilizing sampling rate is dependent on the degree of mismatch between the dynamics of the approximate system and the model used to describe it. This is consistent with the intuition that if the model is exact, the maximum allowable sampling period can be chosen arbitrarily large since the output of the model will match the actual output exactly in this case. Given bounds on the size of the uncertainty, the stability criteria of Proposition 1 can be used to determine the range of stabilizing sampling periods. Alternatively, for a fixed Δ, the maximum tolerable process-model mismatch and the range of stabilizing controller and observer gains can be determined. Note that since $\mathcal{N}_k$ is defined over a finite-dimensional Hilbert space, its spectral radius can be determined from the eigenvalues of $\mathcal{N}_k$.

Remark 2: The idea of using a model to approximate the plant dynamics when measurements are not available has also been used in the context of networked control systems where sensor-controller communication is purposefully suspended to reduce network utilization (e.g., [20], [21], [22]). In these works, however, the sensor-controller communication is limited due to the presence of the network, while in the present work it is limited by the sensor sampling constraints. Moreover, the control architecture presented here differs in that: (1) the controller, observer and model are all collocated, (2) the controller uses the observer state and (3) the model is used by the observer and its state is reset by the plant output (when it is transmitted by the sensor at the sampling times). By contrast, in the architectures presented in [20], [22]: (1) only the controller and model are collocated, while the observer is collocated with the sensor which is on the other side of the network and continuously supplies output measurements to the observer, (2) the controller uses the model state and (3) the model state is reset using the observer state when transmission over the network is allowed.

B. Observer-based fault detection

In this section, we use the fault-free closed-loop behavior characterized in the previous section as the basis for deriving appropriate rules for fault detection and reconfiguration in the system of Eq.10. The idea is to use the state observer in Eq.12 as a fault detection filter and to compare its output with the actual output of the system to determine the health status of the control actuators. The following proposition provides an explicit characterization of the expected fault-free evolution of the residual, which can be used for fault detection.

Proposition 2: *Consider the closed-loop system of Eq.10 and Eq.12, for a fixed $k \in \mathcal{K}$, with $f_a^k \equiv 0$, and consider the augmented system of Eqs.13-14 where the sampling period Δ is chosen such that $r(\mathcal{N}_k(\Delta)) < 1$. Then there exist positive real numbers, $\alpha_k > 1$ and β_k, such that the residual defined by $r_d = \|\bar{y} - \mathcal{Q}\eta\|$ satisfies a time-varying bound of the form $r_d(t) \leq \alpha_k \| \chi_0 \| e^{-\beta_k(t-t_0)}$, for all $t \geq t_0$.*

Proof: Given that $\bar{y} = \mathcal{Q}\bar{x}_s$, and the measurement operator $\mathcal{Q}$ is bounded, it follows that $r_d(t) \leq \|\mathcal{Q}\| \|\bar{x}_s(t) - \eta(t)\| \leq k_1 \|\bar{x}_s(t) - \eta(t)\|$, for some $k_1 > 0$. From the result of Proposition 1, we have that if Δ is chosen such that $r(\mathcal{N}_k(\Delta)) < 1$, then the origin of the augmented system of Eqs.13-14 is exponentially stable, i.e., there exist positive real numbers, $\alpha_1^k > 0$ and β_1^k, such that $\| \chi(t) \| \leq \alpha_1^k \| \chi_0 \| e^{-\beta_1^k(t-t_0)} \| \chi_0 \|$. Since $\|\bar{x}_s(t)\| \leq \|\chi(t)\|$ and $\|\eta(t)\| \leq \|\chi(t)\|$, the following bound can be established on the residual $r_d(t) \leq 2k_1 \alpha_1^k \| \chi_0 \| e^{-\beta_1^k(t-t_0)}$. Setting $\alpha_k = 2k_1\alpha_1^k$ and $\beta^k = \beta_1^k$ completes the proof.

Remark 3: Based on the result of Proposition 2, and for a given stabilizing sampling rate, a fault can be declared at time T_d if the residual breaches the following time-varying threshold:

$$r_d(T_d) > \alpha_k \| \chi_0 \| e^{-\beta_k(T_d - t_0)} \Longrightarrow f_a^k(T_d) \neq 0 \qquad (16)$$

Note, however, that even though η is available continuously, the fact that $\bar{y}$ is available only at the sampling instants implies that the residual can be evaluated only at those times and not continuously, regardless of when the fault actually occurs. While detection delays can be minimized by proper choice of the constants α_k and β_k to ensure that the threshold is sufficiently tight, the smallest possible delay is ultimately constrained by the feasible sampling rate of the measurement sensors.

C. Actuator reconfiguration logic

Once a fault is detected in the operating actuator configuration, the supervisor needs to determine which fall-back configuration to activate in order to preserve closed-loop stability and ensure fault-tolerance. Due to the dependence of the operator Λ_k on the input operator $\mathcal{B}_s^k$ (which is parameterized by the locations of the control actuators), the maximum allowable sampling period is dependent on the choice of the control actuator location. Using the result of Proposition 1, for a given sampling period, feedback and observer gains, the stabilizing actuator locations can be determined. This determination constitutes the basis for the actuator reconfiguration logic given in Theorem 1 below. The proof follows directly from the result of Proposition 1 and is omitted for brevity.

Theorem 1: *Consider the closed-loop system of Eq.10 and Eq.12, with $k(0) = i$ for some $i \in \mathcal{K}$ and a sampling period Δ such that $r(\mathcal{N}_i(\Delta)) < 1$. Let T_f be the earliest time that $f_a^i(T_f) \neq 0$. Then the following switching rule:*

$$k(t) = \left\{ \begin{array}{ll} i, & 0 \leq t < T_f \\ \nu \neq i, & t \geq T_f,\ r(\mathcal{N}_\nu(\Delta)) < 1 \end{array} \right\} \qquad (17)$$

exponentially stabilizes the origin of the closed-loop system.

Remark 4: The switching logic in Theorem 1 ensures that the control system switches to a stabilizing actuator configuration for the given sampling period in the absence of faults. While Theorem 1 considers the case of a single fault, the same logic applies in the case of multiple consecutive faults. Note also that the structure of the operator Λ_k changes after each actuator switching; therefore, a new residual threshold should be used following each actuator switching to allow for the detection of future faults.

IV. Implementation of FD-FTC architecture on the infinite-dimensional system

In this section, we describe how the controller, fault detection filter and actuator switching logic designed in Section III are implemented using the measured output of the infinite-dimensional system and the necessary modifications needed to maintain the desired fault-tolerance properties.

A. Feedback controller implementation

When considering measurements of the output of the infinite-dimensional system of Eq.9, the output feedback controller can be implemented as follows:

$$\begin{array}{rcl} u(t) & = & \mathcal{F}^k \eta(t),\ t \in [t_j, t_{j+1}) \\ \dot{w}(t) & = & \widehat{\mathcal{A}}_s w(t) + \widehat{\mathcal{B}}_s^k u(t) \\ \dot{\eta}(t) & = & (\widehat{\mathcal{A}}_s - \mathcal{L}\mathcal{Q}) x_s(t) + \widehat{\mathcal{B}}_s^k u(t)\ +\ \mathcal{L} y(t) \\ w(t_j) & = & \mathcal{Q}^{-1} y(t_j),\ j = 0, 1, 2, \cdots \end{array} \qquad (18)$$

which is similar to the controller of Eq.12 except that the output y (instead of $\bar{y}$) is used to implement the observer and update the state of the model of the finite-dimensional slow subsystem (notice that x_s is unknown and thus the entire output must be used in updating the state of the model). Defining the error variable $e_s = w - x_s$, where $e_s \in \mathcal{H}_s$ is the difference between the model-generated estimate of the slow state and the actual slow state, and introducing the augmented state $\chi = [x_s\ \eta\ e_s]'$, it can be shown that the augmented slow subsystem can be formulated as:

$$\begin{array}{rcl} \dot{\chi}(t) & = & \Lambda_k \chi(t) + \mathcal{G} x_f,\ \ t \in (t_j, t_{j+1}) \\ e_s(t_j) & = & x_f,\ \ j = 0, 1, 2, \cdots, \end{array} \qquad (19)$$

where Λ_k is given by Eq.14 and $\mathcal{G} = [0\ \mathcal{L}\mathcal{Q}\ 0]'$. Note that as a result of using the output of the infinite-dimensional system (which contains both the slow and the fast states), the evolution of the augmented system is now influenced by x_f. Furthermore, the model estimation error cannot be reset to zero exactly at the sampling instants. The following proposition provides a stability condition for the infinite-dimensional sampled-data closed-loop system that ties the sampling period with the separation between the slow and fast eigenvalues of $\mathcal{A}$, $\epsilon = |\lambda_m|/|\lambda_{m+1}|$. The proof of the proposition can be obtained using singular perturbation arguments [3] and is omitted for brevity.

Proposition 3: *Consider the infinite-dimensional system of Eqs.7-9, with $f_a^k \equiv 0$, subject to the controller and update law of Eq.18. Then, if $r(\mathcal{N}_k(\Delta)) < 1$, where $\mathcal{N}_k(\Delta)$ was defined in Proposition 1, there exists a positive real number ϵ^* such that if $\epsilon \in (0, \epsilon^*]$, the zero solution of the infinite-dimensional closed-loop system is exponentially stable.*

Remark 5: According to the result of Proposition 3, a sampling period that stabilizes the approximate finite-dimensional fault-free system of Eq.19 with $x_f = 0$ continues to stabilize the infinite-dimensional system provided that the separation between the slow and fast eigenvalues is sufficiently large (an estimate of ϵ^* can be obtained using singular perturbation analysis). This restriction, which requires that a sufficient number of slow states and measurements be included in the controller design, is needed to ensure that the error introduced by updating the model state using $\mathcal{Q}^{-1} y$ (rather than x_s) is sufficiently small. Notice also that, unlike the finite-dimensional case, the evolution of the augmented slow subsystem of Eq. 19 is dependent on x_f. In the limit as $\epsilon \to 0$, this coupling disappears.

B. Actuator fault detection and reconfiguration

When the slow state observer in Eq.18 is used to detect faults in the infinite-dimensional system, its output has to be compared against the actual output y (since it is y, not $\bar{y}$, that is available for measurement in the infinite-dimensional setting). This motivates re-defining the residual as $r_d = \|y - \mathcal{Q}\eta\|$. Unlike the residual in the finite-dimensional case, this residual depends on both x_s and x_f, and is therefore sensitive not only to faults but also to approximation errors (made by neglecting x_f when deriving the approximate finite-dimensional system). To prevent false alarms due to these errors, it is important to establish a bound on the residual which captures its expected behavior in the absence of faults. This bound is established in the following proposition and can be used by the supervisor as an alarm threshold to decide when a fault can be declared and consequently when to switch actuator configurations.

Proposition 4: *Consider the infinite-dimensional system of Eqs.7-9, with $f_a^k \equiv 0$, subject to the controller and update law of Eq.18 where the sampling period Δ is chosen such that $r(\mathcal{N}_k(\Delta)) < 1$. Then given any pair of positive real numbers $(d, T_b > t_0)$, there exists a positive real number $\widehat{\epsilon}$ such that the residual $r_d = \|y - \mathcal{Q}\eta\|$ satisfies:*

$$r_d(t) \leq \alpha_k \|\, \chi_0 \,\| e^{-\beta_k (t - t_0)} + d,\ \forall\, t \geq T_b$$

Proof: From Proposition 3, we have that the origin of the closed-loop system of Eqs.7-9 and Eq.18 (with $f_a^k \equiv 0$) is exponentially stable for $\epsilon \in (0, \epsilon^*]$. This implies the existence of $\epsilon_s > 0$ such that, for $\epsilon \in (0, \epsilon_s]$, the solution of the x_s-subsystem of Eq.7 satisfies $\|x_s(t) - \bar{x}_s(t)\| \leq k_1 \epsilon$

for all $t \geq 0$, for some $k_1 > 0$. Furthermore, given any $T_b > t_0$, there exists $\epsilon_f > 0$, such that for $\epsilon \in (0, \epsilon_f]$, the solution of the x_f-subsystem of Eq.8 satisfies $\|x_f(t)\|_2 \leq k_2\epsilon$ for all $t \geq T_b$, for some $k_2 > 0$. Re-writing $r(t) = \|y - \mathcal{Q}\eta\| \leq \|y - \bar{y}\| + \|\bar{y} - \mathcal{Q}\eta\|$, and using the fact that $\|\bar{y} - \mathcal{Q}\eta\| \leq \alpha_k\|\chi_0\|e^{-\beta_k(t-t_0)}$ when $f_a^k = 0$ (from Proposition 2), we have $r(t) \leq \|\mathcal{Q}\|\|x_s - \bar{x}_s\| + \|\mathcal{Q}\|\|x_f(t)\|_2 + \alpha_k\|\chi_0\|e^{-\beta_k(t-t_0)} \leq k_3\epsilon + \alpha_k\|\chi_0\|e^{-\beta_k(t-t_0)}$ for all $[T_b, \infty)$, where $k_3 = (k_1 + k_2)\|\mathcal{Q}\| > 0$. Finally, given any $d > 0$, there exists $\widehat{\epsilon} := \min\{d/k_3, \epsilon_s, \epsilon_f\}$ such that for $\epsilon \leq \widehat{\epsilon}$, $r_d(t) \leq \| \chi_0 \|\alpha_k e^{-\beta_k(t-t_0)} + d$, for all $t \geq T_b$.

Remark 6: Proposition 4 prescribes two modifications to the fault detection rules described in the finite-dimensional case. These include (1) enlarging the detection threshold by a certain amount, $d = O(\epsilon)$, that reflects the size of the approximation error, and (2) evaluating the residual only after a small period of time $[0, T_b]$ has elapsed to ensure that x_f (i.e., the approximation error) has converged sufficiently close to zero. Notice that both d and T_b can be chosen arbitrarily small provided that ϵ is sufficiently small.

Remark 7: Similar to the way that the feedback controller and fault detection filter are implemented, one can show using singular perturbation arguments that the actuator reconfiguration logic of Eq.17 which is based on the approximate finite-dimensional system continues to enforce closed-loop stability in the infinite-dimensional system provided that ϵ is sufficiently small.

V. Simulation study: Fault-tolerant stabilization of a diffusion-reaction process

To illustrate the application of the fault detection and fault-tolerant control methodology described earlier, we consider a linearized diffusion-reaction process of the form:

$$\frac{\partial \bar{x}}{\partial t} = \frac{\partial^2 \bar{x}}{\partial z^2} + \left(\beta_T \gamma e^{-\gamma} - \beta_U\right)\bar{x} + \beta_U b(z)[u(t) + f_a(t)]$$

subject to the boundary and initial conditions of Eq.4, where $\bar{x}$ denotes a dimensionless temperature, β_T denotes a dimensionless heat of reaction, γ denotes a dimensionless activation energy, β_U denotes a dimensionless heat transfer coefficient, u denotes the temperature of the cooling medium, f_a is an actuator fault, and $b(z)$ denotes the actuator distribution function. For typical values of the process parameters, $\beta_T = 50.0$, $\beta_U = 2.0$, $\gamma = 4.0$, the operating steady state $\bar{x}(z,t) = 0$ is open-loop unstable. The control objective is to stabilize the temperature profile at this unstable steady state by manipulating the temperature of the cooling medium, $u(t)$, in the presence of actuator faults. We consider the first eigenvalue as the dominant one and use standard Galerkins method to derive an ODE that describes the temporal evolution of the amplitude of the first eigenmode: $\dot{a}_1 = \lambda_1 a_1 + g(z_a)u$, where $\bar{x}(z,t) = \sum_{i=1}^{\infty} a_i(t)\phi_i(z)$, $g(z_a) = \beta_u\langle\phi_1(z), b(z)\rangle$, and a single point actuator (with finite support) is used for stabilization, i.e., $b(z) = 1/(2\mu)$ for $z \in [z_a - \mu, z_a + \mu]$, where μ is a sufficiently small number, and $b(z) = 0$ elsewhere. This ODE is used to design the output feedback controller and fault detection filters which are then implemented on a 30-th order Galerkin discretization of the PDE (higher order discretizations led to identical results).

Following the methodology outlined in Section III, we consider an output feedback controller of the form: $u = F\eta$, where F is the feedback gain, η is an estimate of a_1 generated by an observer of the form $\dot{\eta} = (\widehat{\lambda}_1 - LQ_s(z_s))\eta + \widehat{g}(z_a)u + Ly$ from the measured output, $y(t) = \langle q(z - z_s), \bar{x}(z,t)\rangle$, provided by a point sensor located at $z = z_s$, where $Q_s(z_s) = \langle q(z - z_s), \phi_1(z)\rangle$, $q(z - z_s)$ is the sensor distribution function, and the observer gain L is chosen so that $\widehat{\lambda}_1 - LQ_s(z_s) < 0$. Following the analysis presented in Section IV, it can be verified that the closed-loop system is exponentially stable if an only if the eigenvalues of the matrix $N_k(\Delta) = I_o e^{\Lambda_k \Delta} I_o$ are inside the unit circle, where:

$$\Lambda_k = \begin{bmatrix} \lambda_1 & g(z_a^k)F^k & -g(z_a^k)F^k \\ LQ_s(z_s) & \widehat{\lambda}_1 + \widehat{g}(z_a^k)F^k - LQ_s(z_s) & LQ_s(z_s) \\ \widehat{\lambda}_1 - \lambda_1 & [\widehat{g}(z_a^k) - g(z_a^k)]F^k & \widehat{\lambda}_1 \end{bmatrix}$$

and $I_o = \text{diag}\,[1\ 1\ 0]$. Since closed-loop stability requires all the eigenvalues of N_k to lie within the unit circle, it is sufficient to consider only the maximum eigenvalue magnitude. We consider first the case when no faults are present in the operating actuator configuration, and analyze the dependence of closed-loop stability on the selection of the actuator location and sampling period. Fig.1 (left) is a contour plot showing the dependence of the maximum eigenvalue magnitude on both the position of the actuator, z_a, and the sampling period, Δ, when an uncertain model (with $\widehat{\lambda}_1 = 0.3$ and $\widehat{g}(z_a) = 0.5$) is used to estimate the evolution of a_1 between sampling instances, and the output feedback controller is designed with constant controller and observer gains, $F = -15$ and $L = 100$, respectively. The area enclosed by the unit contour line represents the stability region for the closed-loop system. It can be seen that (1) the set of stabilizing actuator locations increases as the sampling period decreases and (2) the maximum stabilizing sampling period shrinks as the actuator is moved closer to the middle. This result can be explained by the fact that when all actuator locations share the same feedback gain, the closed-loop response in the absence of sampling $\dot{a}_1 = (\lambda_1 + g(z_a)F)a_1$ is fastest at the middle location (where the first eigenfunction has a maximum) and therefore more frequent sampling is needed at this location when the measurements are not available continuously. For comparison, the area enclosed by the unit contour lines in Fig.1 (right) represents the stability region when a sample-and-hold scheme (i.e., a model of the form $\dot{w}(t) = 0$, $t \in (t_j, t_{j+1})$) is used. The stable region is slightly smaller in this case. In general, however, if the plant-model mismatch is too large, the sample-and-hold scheme may outperform the model-based scheme.

To illustrate the fault detection and handling capabilities of the sampled data control system, the process is initialized using a healthy actuator placed at $z_a = 0.25$ and the

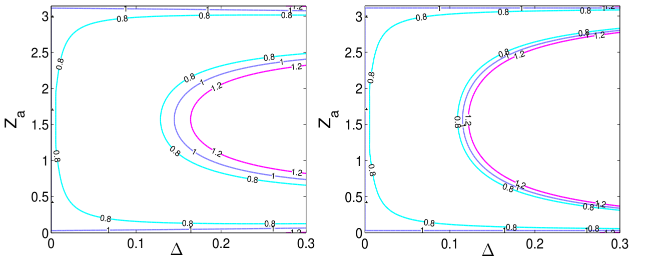

Fig. 1. Dependence of the maximum eigenvalue magnitude of N on the sampling period and actuator location under a model update scheme (left) and a sample-and-hold scheme (right).

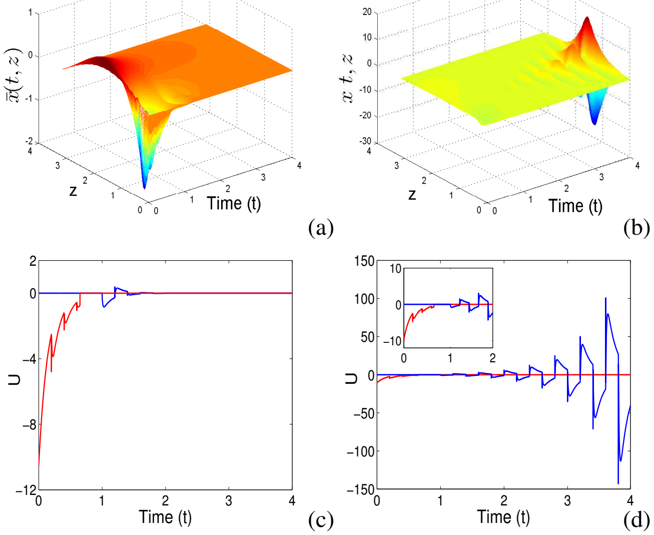

Fig. 2. Evolution of the closed-loop state profiles (top) and manipulated input profiles (middle) when a fault is detected in the primary actuator and subsequent reconfiguration to an actuator placed at $z_a = 0.6$ (a,c) and to an actuator at $z_a = 1.3$ (b,d) takes place.

sampling period is set at $\Delta = 0.2$. Based on the evolution of the residual in the absence of faults, we choose a detection threshold of $\delta = 0.04$ for $T_f \geq T_b = 0.5$. This allows sufficient time for the fast modes to converge. At $T_f = 0.65$, a fault is introduced in the operating actuator (see the red line in Fig.2(c)). The residual profile in Fig.3(a) shows that the fault is detected at $T_d = 1.0$ when it causes the residual to breach the threshold. At this time, the supervisor needs to switch to a backup actuator to maintain closed-loop stability. For the given sampling period, Fig.1(left) indicates that the actuator placed at $z_a = 0.6$ lies inside the unit contour zone and is therefore expected to be stabilizing, while the actuator placed at $z_a = 1.3$ lies outside and therefore cannot stabilize the close-loop system. This prediction is confirmed by the closed-loop state profiles in Fig.2(a-b). The blue lines in Figs.2(c-d) depict the manipulated input profiles for the backup actuators.

References

[1] W. Ray, *Advanced Process Control*. New York: McGraw-Hill, 1981.

[2] P. D. Christofides and P. Daoutidis, "Finite-dimensional control of parabolic PDE systems using approximate inertial manifolds," *J. Math. Anal. Appl.*, vol. 216, pp. 398–420, 1997.

[3] P. D. Christofides, *Nonlinear and Robust Control of PDE Systems: Methods and Applications to Transport-Reaction Processes*. Boston: Birkhäuser, 2001.

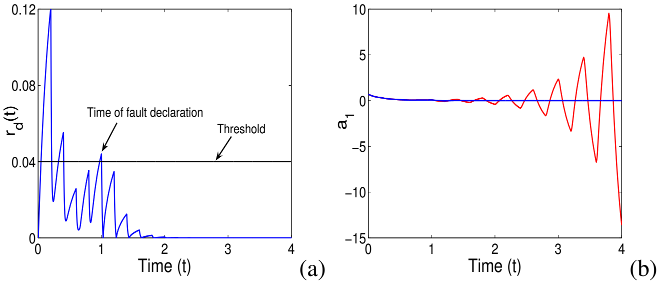

Fig. 3. (a) Evolution of the residual when a fault is introduced at $T_f = 0.65$ in the primary actuator and subsequent reconfiguration to an actuator placed at $z_a = 0.6$ takes place. (b) Evolution of the amplitude of the first eigenmode when the actuator placed at $z_a = 0.6$ (blue) is activated following fault detection and when the actuator placed at $z_a = 1.3$ (red) is activated instead.

[4] A. Alonso and B. E. Ydstie, "Stabilization of distributed systems using irreversible thermodynamics," *Automatica*, vol. 37, pp. 1739–1755, 2001.

[5] M. Demetriou and N. Kazantzis, "A new actuator activation policy for performance enhancement of controlled diffusion processes," *Automatica*, vol. 40, pp. 415–421, 2004.

[6] M. Krstic, "Systematization of approaches to adaptive boundary control of PDEs," *Inter. J. Rob. Nonlin. Contr.*, vol. 16, pp. 801–818, 2006.

[7] D. M. Himmelblau, *Fault Detection and Diagnosis in Chemical and Petrochemical Processes*. New York: Elsevier Scientific Pub., 1978.

[8] P. M. Frank and X. Ding, "Survey of robust residual generation and evaluation methods in observer-based fault detection systems," *J. Proc. Contr.*, vol. 7, pp. 403–424, 1997.

[9] C. DePersis and A. Isidori, "A geometric approach to nonlinear fault detection and isolation," *IEEE Trans. Automat. Contr.*, vol. 46, pp. 853–865, 2001.

[10] S. Simani, C. Fantuzzi, and R. Patton, *Model-based Fault Diagnosis in Dynamic Systems Using Identification Techniques*. London: Springer, 2003.

[11] M. Blanke, M. Kinnaert, J. Lunze, and M. Staroswiecki, *Diagnosis and Fault-Tolerant Control*. Berlin-Heidelberg: Springer, 2003.

[12] L. Cheng, E. Kwok, and B. Huang, "Closed-loop fault detection using local approach," *Can. J. Chem. Eng.*, vol. 81, pp. 1101–1108, 2003.

[13] V. Venkatasubramanian, R. Rengaswamy, K. Yin, and S. N. Kavuri, "Review of process fault diagnosis - parts I, II, III," *Comp. & Chem. Eng.*, vol. 27, pp. 293–346, 2003.

[14] H. Baruh, "Actuator failure detection in the control of distributed systems," *Journal of Guidance, Control, and Dynamics*, vol. 9, pp. 181–189, 1986.

[15] A. Armaou and M. Demetriou, "Robust detection and accommodation of incipient component and actuator faults in nonlinear distributed processes," *AIChE J.*,, vol. 54, pp. 2651–2662, 2008.

[16] N. H. El-Farra and P. D. Christofides, "Coordinating feedback and switching for control of spatially-distributed processes," *Comp. & Chem. Eng.*, vol. 28, pp. 111–128, 2004.

[17] N. H. El-Farra, "Integrated fault detection and fault-tolerant control architectures for distributed processes," *Ind. & Eng. Chem. Res.*, vol. 45, pp. 8338–8351, 2006.

[18] N. H. El-Farra and S. Ghantasala, "Actuator fault isolation and reconfiguration in transport-reaction processes," *AIChE J.*, vol. 53, pp. 1518–1537, 2007.

[19] S. Ghantasala and N. H. El-Farra, "Robust fault detection and handling in uncertain transport-reaction processes," *Dynam. Contin. Dis. & Impul. Syst. (Series A)*, vol. 14, pp. 203–208, 2007.

[20] L. A. Montestruque and P. J. Antsaklis, "On the model-based control of networked systems," *Automatica*, vol. 39, pp. 1837–1843, 2003.

[21] Y. Sun and N. H. El-Farra, "Quasi-decentralized model-based networked control of process systems," *Comp. & Chem. Eng.*, vol. 32, pp. 2016–2029, 2008.

[22] ——, "Quasi-decentralized state estimation and control of process systems over communication networks," in *Proceedings of 47th IEEE Conference on Decision and Control*, Cancun, Mexico, 2008, pp. 5468–5475.